frontiers | Frontiers in Environmental Science

TYPE Original Research
PUBLISHED 18 April 2024
DOI 10.3389/fenvs.2024.1358297

OPEN ACCESS

EDITED BY
Amin Mojiri,
Arizona State University, United States

REVIEWED BY
Meifang Li,
Central South University Forestry and Technology, China
Shaohua Wu,
Guangdong University of Petrochemical Technology, China

*CORRESPONDENCE
Hui Jiang,
jianghui1368@163.com
Da Sun,
sunday@wzu.edu.cn

RECEIVED 19 December 2023
ACCEPTED 25 March 2024
PUBLISHED 18 April 2024

CITATION
Huang Y, Yang Q, Song L, Ran H, Jiang H and Sun D (2024), Efficient eradication of organotin utilizing K_2FeO_4 augmented by nZVI: revelations on influential factors, kinetic dynamics, and mechanistic insights. *Front. Environ. Sci.* 12:1358297. doi: 10.3389/fenvs.2024.1358297

Efficient eradication of organotin utilizing K_2FeO_4 augmented by nZVI: revelations on influential factors, kinetic dynamics, and mechanistic insights

Yuanyuan Huang[1,2], Qingwei Yang[1], Ling Song[3], Hongjie Ran[1], Hui Jiang[1]* and Da Sun[4]*

[1]School of River and Ocean Engineering, Chongqing Jiaotong University, Chongqing, China, [2]Chongqing Academy of Science and Technology, Chongqing, China, [3]Chongqing Water Group Co., Ltd., Chongqing, China, [4]Zhejiang Pro-Vincial Key Laboratory for Water Environment and Marine Biological Resources Protection, National and Local Joint Engineering Research Center for Ecological Treatment Technology of Urban Water Pollution, Institute of Life Sciences and Biomedical Collaborative Innovation Center of Zhejiang Province, Wenzhou University, Wenzhou, China

In this study, we investigated the oxidative mechanisms of nano zero-valent iron (nZVI) enhanced potassium ferrate (K_2FeO_4), focusing on tributyltin (TBT) and triphenyltin (TPhT) as target pollutants. The addition of nZVI enhanced the degradation of both organic tin compounds by K_2FeO_4, exhibiting pseudo-first-order kinetics influenced by pH, carbonate, and fulvic acid. nZVI, as a reducing agent, facilitated the generation of stronger oxidizing species Fe (V) and Fe (IV) from K_2FeO_4 through electron transfer. The presence of hydroxyl radicals (OH) was confirmed by tert-butyl alcohol (TBA) verification. Intermediate products of TBT degradation by nZVI-enhanced K_2FeO_4 were identified using GC-MS, confirming de-alkylation leading to stepwise oxidation to inorganic tin ions. Due to excessively long Sn-C bonds in diphenyltin, rendering them unstable, Density Functional Theory (DFT) calculations were employed. Results indicated that Fe (IV) and Fe (V) predominantly attacked the Sn-C bonds of TPhT, while OH primarily targeted the benzene ring. HOMO energy levels suggested that Fe (V) was more prone to oxidizing TPhT than Fe (IV). Gibbs free energy calculations demonstrated that, in the presence of Fe (IV) and Fe (V), the energy barrier for breaking bonds and oxidizing into inorganic tin ions decreased, favoring the process over the self-decomposition of TPhT. Additionally, the lower energy barrier for OH indicated an easier degradation of TPhT. This study reveals that nZVI-enhanced K_2FeO_4 effectively removes TBT and TPhT, contributing to the understanding of the ferrate-mediated degradation mechanism of organic tin compounds. The findings offer insights and theoretical guidance for remediating organic tin pollution in aquatic environments.

KEYWORDS

potassium ferrate, nano zero-valent iron, water environment, organic tin, removal effect

1 Introduction

Organotin compounds find extensive applications in various sectors such as PVC stabilizers (Xu et al., 2022), agricultural pesticides (Xiao et al., 2013), wood preservation (Hu et al., 2020), antifouling coatings for ships (Du et al., 2014), and antifouling biocides (Ribas et al., 2020); The widespread usage of organotin has led to water environment pollution, causing disruptions in the reproductive systems of gastropods, resulting in sexual distortions and other malformations in mollusks (de Carvalho Oliveira and Santelli, 2010; Pagliarani et al., 2013). Additionally, it induces immunotoxicity, neurotoxicity, mutagenicity, and carcinogenicity in humans (Fent, 1996), contributing to diseases related to fertility and immune function. Among the 67 endocrine disruptors published by the U.S. Environmental Protection Agency (USEPA), TBT and TPhT are the only two organometallic compounds, and are the most hazardous and have the widest impact area among organotins (Gao et al., 2004). Although many countries and international organizations have established safety standards for TBT and TPhT and imposed restrictions on their use (Chen, 2019), their presence is still detected in various water environments such as oceans, rivers, and lakes (Chen et al., 2019). The current treatments related to organotin include biological (Hassan et al., 2019; Song et al., 2020), physical (Chang EE. et al., 2012), and chemical (Sakultantimetha et al., 2010) methods, which can gradually reduce the toxicity of organotin. Stasinakis et al. (2005) employed the activated sludge method in a batch reactor for the biodegradation of organotin compounds. Their research revealed that almost all organic tin compounds were removed from the dissolved phase and accumulated on suspended solids 1 day after the addition of organic tin. Over the subsequent 18 days, the particulate fraction of organic tin compounds underwent a series of dealkylation processes, thereby undergoing biodegradation. Chang E-E. et al. (2012) discovered that under well-controlled conditions such as calcium ions, humic acid, and pH, the nanofiltration membrane achieved a retention rate of over 85% for mono-, di-, and tributyltin in water. Brosillon et al. (2014) demonstrated that through ultraviolet (UV) irradiation and titanium dioxide (TiO_2) catalyst, the degradation rate of TBT in aqueous solution could reach 99.8% within 30 min, whereas under UV irradiation alone, the degradation rate was only 10%. However, photolysis requires exposure to ultraviolet light, making organic tin less susceptible to photodegradation in deep water and sediment. From the foregoing analysis, it is evident that methods for the degradation of organic tin compounds are susceptible to external conditions, leading to unstable effluent quality, long treatment cycles, and inapplicability in certain scenarios. Consequently, seeking an efficient and environmentally friendly treatment method is crucial for effectively addressing organic tin compounds.

Pertechnate is a new type of highly efficient multifunctional water treatment agent integrating "oxidation, adsorption, flocculation, coagulation aid, deodorization, and sterilization" (Wu et al., 2020), but as an oxidizing agent, coagulant and disinfectant alone, it is not an effective in the removal of some organic or inorganic pollutants. In recent years, based on photocatalysis, aluminum salts, ozone, hypochlorite (sulfite) and other combined technology research has been paid attention to, and the analysis of the combined effect on the treatment of pollutants has been significantly enhanced, mainly through the enhancement of flocculation, oxidation, and the generation of oxidizing free radicals and oxidation of the extension of the time to enhance the oxidation of pollutants removal effect (Chen, 2012; Han et al., 2013; Liu et al., 2019; Zhu et al., 2019; Tian et al., 2020; Yuan et al., 2020). Zero-valent iron has been widely used in water treatment in recent years due to its active nature and abundant content, and is often used as a reducing agent for the remediation of water pollution (Tepong-Tsindé et al., 2015). Investigation into the removal efficiency of para-nitrophenol (PNP) utilizing ozone and nano zero-valent iron unveiled that their combined application significantly augmented PNP removal compared to their individual use (Xiong et al., 2016). In addition, the combination of nZVI and K_2FeO_4 not only promotes the production of more oxidizing Fe^{5+} and Fe^{4+} by K_2FeO_4, but also generates micron- or nanoscale colloids by itself, which removes pollutants from the water body through adsorption and precipitation mechanisms, while not causing secondary pollution to the environment.

Previous studies have indicated that the Sn-C bond in organotin undergoes nucleophilic or electrophilic attacks leading to cleavage, but the mechanism of its reaction with Fe (VI) remains unclear (Hoch, 2001). Furthermore, detailed elucidation of each individual reaction step is challenging based on thermodynamic and kinetic experiments. DFT calculations offer a possibility to interpret complex reaction processes (Li et al., 2021). Through DFT calculations, Wang et al. (2018) investigated the impact of pollutant substitution positions (ortho, meta, and para) on degradation rates. Calculations based on Frontier Molecular Orbital theory help identify the most reactive sites in the target compounds. Cao et al. (2015) explored the reactivity of pollutants through Highest Occupied Molecular Orbital (HOMO) and Lowest Unoccupied Molecular Orbital (LUMO) values. Calculation of transition state theory and reaction barriers can determine preferred reaction pathways, crucial for a deeper understanding of the reaction mechanism (Wu et al., 2023). However, despite the widespread application of theoretical computational methods, a systematic investigation into the removal mechanisms of TBT and TPhT by nZVI-enhanced Fe (VI) has yet to be conducted.

Based on the above analysis, nZVI enhanced K_2FeO_4 technology was used to investigate the effect of degradation and removal of TBT and TPhT, and the main discussions are as follows: 1) to study the effects of K_2FeO_4 and nZVI dosing ratio and pH on the removal of organotin and the kinetics of the reaction on the removal of organotin; 2) to discuss the efficiency of the removal of organotin in simulated real water bodies by K_2FeO_4 and nZVI; 3) The reaction mechanism of organotin removal by K_2FeO_4 and nZVI was explored by free radical verification, theoretical calculation and GC-MS intermediate product detection. This study is expected to provide a reference for the removal of organotin in actual water.

2 Materials and methods

2.1 Reagents and instruments

The reagents, including tributyltin chloride ($C_{12}H_{27}SnCl$, 96%), triphenyltin chloride ($C_{18}H_{15}ClSn$, 96%), potassium ferrate

(K_2FeO_4, Analytical Reagent), nano zero-valent iron (nZVI), sodium tetraethylborate ($C_8H_{20}BNa$, 98%), cyclohexen-3-one phenol ketal ($C_7H_6O_2$, 98%), sodium hydroxide (NaOH, 96%), methanol (CH_3OH, 99.5%), hexane (C_6H_{14}, 97%), tetrahydrofuran (C_4H_8O, Analytical Reagent), and tert-butanol (TBA, ≥99%), were all purchased from Aladdin Reagent Co., Ltd. (Shanghai, China). Unless otherwise specified, all solutions were prepared using Milli-Q water.

The experimental setup involved instruments such as gas chromatography-mass spectrometry apparatus (GCMS-QP2010, Shimadzu, Japan), ultrapure water preparation system (Milli-Q Advanced, Millipore Corporation, United States), magnetic stirrer (HJ-6A, Guohua Electric Company, China), and precision pH meter (PHS-25, Leici, China).

2.2 Degradation of K_2FeO_4 with nZVI for the removal of TBT and TPhT

Derivatization-liquid-liquid extraction-gas chromatography/mass spectrometry (GC/MS) was employed for the determination of organotin compounds, which were meticulously and precisely quantified within the aqueous medium. These compounds were extracted from a minute volume of 0.2 mL, falling within the linear range of 25–2,500 μg/L (Wang et al., 2013). Coupled with the optimal elimination rate of organotin, the task was to precisely gauge the residual organotin concentration. Accordingly, initial concentrations of the two organotins were set at 500 μg/L each, whereupon 100 mL of solution was measured into a conical flask for readiness. The temperature was maintained at 25°C, with a rotational speed of 200 r/min, and sampling occurred every 10 min to ascertain the remaining concentration.

In the K_2FeO_4 and nZVI dosage ratio exploration, a pH of 8 was stipulated. For TBT and TPhT solutions, 100 mg/L of K_2FeO_4 was introduced, with nZVI dosages added in proportions of 1:0, 1:0.8, 1:1, 1:2, and 1:3, correspondingly. Moreover, in the TPhT solution, 100 mg/L of nZVI was supplemented, with K_2FeO_4 to nZVI ratios established at 1:1, 2:1, 3:1, and 4:1. In the pH investigation, TBT and TPhT solutions underwent treatment with concentrations of 100 and 300 mg/L of K_2FeO_4, while the nZVI dosage was maintained at 100 mg/L. Nitric acid was utilized to modulate the pH to 3.5, 6.5, 8.0, 9.0, and 10.0. In both the free radical quenching and simulated real water experiments, the doses of K_2FeO_4 and nZVI mirrored those in the pH study. For TBT and TPhT solutions, TBA was introduced at concentrations of 0, 1, 10, and 50 mg/L; sodium carbonate at concentrations of 0, 5, 10, 20, and 40 mg/L; and humic acid at concentrations of 0, 1, 5, 10, and 20 mg/L. Samples were collected subsequent to the culmination of the oscillating reactions for the assessment of residual organotin concentrations.

2.3 Detection method for organotin compounds

The sample separation and enrichment were conducted using a derivatization-liquid-liquid extraction approach. Initially, 200 μL of water sample was taken in a 1.5 mL extraction vial, to which 200 μL of acetic acid-sodium acetate buffer solution with a pH of 4.2 was added to adjust the pH to acidic conditions. Subsequently, 40 μL of 2% sodium tetrahydroborate derivatization reagent was introduced for derivatization, and 200 μL of 3% cyclohexenone in n-hexane extraction agent was added to enhance extraction efficiency. The vial was then sealed, shaken for 4 min, and left to stand for 3 min. After the phase separation of aqueous and organic phases, the organic phase solution was collected.

Finally, the upper layer of the organic solution was analyzed using gas chromatography-mass spectrometry (GC-MS). The gas chromatography conditions included a DB-5 ms column (30 m × 0.25 mm, 0.25 μm), constant flow with no split injection, a flow rate of 1.5 mL/min, an injector temperature of 250°C, and an injection volume of 2 μL. The temperature program involved an initial temperature of 70°C, ramping at 10°C/min to 220°C with a 1-min hold, followed by a further increase at 25°C/min to 280°C with a 20-min hold.

The gas chromatography-mass spectrometry conditions comprised an electron ionization (EI) ion source with a temperature of 230°C, an interface temperature of 250°C, a solvent delay of 3 min, and an ionization energy of 70 eV.

2.4 Calculation method

2.4.1 Calculation of removal efficiency for TBT and TPhT

$$\textit{Removal Efficiency} = \frac{C_0\text{-}C_1}{C_0} \times 100\% \quad (1)$$

In the equation: C_0 represents the initial concentration of TBT or TPhT, and C_1 represents the residual concentration of TBT or TPhT.

2.4.2 Reaction kinetics calculation

The oxidative degradation of TBT and TPhT by K_2FeO_4 with nZVI was fitted with quasi-primary reaction kinetics to investigate the kinetic equations of TBT and TPhT under the conditions of different dosing ratios as follows:

$$\frac{dC_0}{d_t} = -k_{obs}[C] \quad (2)$$

Integration of Eq. 2 yields:

$$ln\frac{[C]_0}{[C]} = k_{obs}t + b \quad (3)$$

Where: $k_{obs} = k\,[K_2FeO_4]$: quasi-primary reaction rate constant, s^{-1}; $[C]_0$: initial reaction concentration of TBT or TPhT; b: integration constant.

2.5 Theoretical calculation

The Gibbs free energy is computable through DFT utilizing the CASTEP software package, as implemented in Materials Studio (Wang et al., 2019; Bouakline et al., 2023; Liu et al., 2023). The calculations employ the Generalized Gradient Approximation (GGA) in conjunction with the Perdew–Burke–Ernzerhof (PBE)

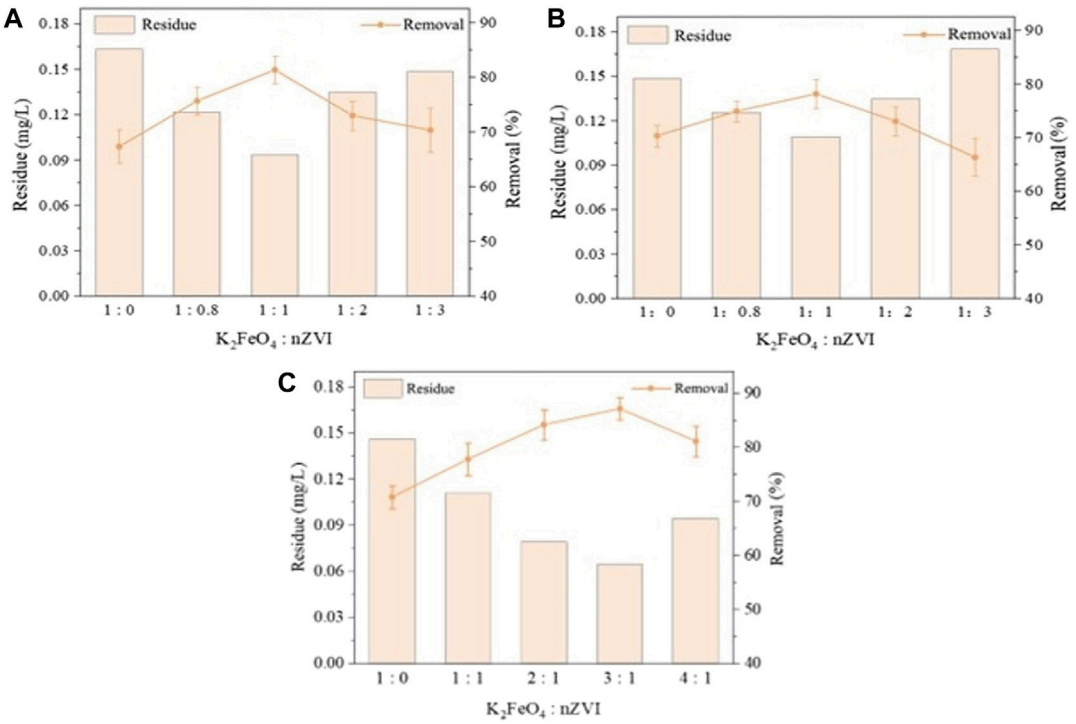

FIGURE 1
Investigation of the impact of varied nZVI dosages on the removal of TBT and TPhT **(A,B)**, and the influence of different K_2FeO_4 dosages on TPhT removal efficiency **(C)**.

pseudopotential for handling exchange-correlation energies. The convergent cutoff energy is set to 400 eV, and the HOMO and LUMO are computed using the Dmol3 code. Prior to energy calculations, geometric optimization is performed for all atomic models. Additionally, a double numerical plus polarization (DNP) basis set is considered, with convergence tolerances set at 0.054 eV/Å, 0.00136 eV, and 0.005 Å for gradients, energy, and displacements, respectively.

3 Results

3.1 Effect of K_2FeO_4 and nZVI dosage on the removal of organotin

The degradation rates of TBT and TPhT were enhanced to different degrees by adding different ratios of nZVI reductant compared with the addition of K_2FeO_4 alone (Figures 1A, B). With the increase of nZVI dosage, the removal of two kinds of organotin firstly increased and then decreased, and reached a maximum of 81.6% and 78.0% for TBT and TPhT, respectively, at the dosage ratio of 1:1. Under the condition of the same speciation ratio, the removal rate of TPhT was lower than that of TBT. According to the mechanism analysis in Section 2.5, it is known that the degradation process of TPhT generates substances such as phenol, which increases the consumption of high-valent iron and reduces the removal effect of TPhT. Therefore, more oxidizing ions were generated by increasing the K_2FeO_4 dosage to increase the removal rate of TPhT, and the results are shown in Figure 1C. With the increase of K_2FeO_4 dosage, the removal rate of TPhT increased, indicating that the generated intermediates were effectively degraded. When the dosing ratio was 3:1, the removal effect of TPhT was optimized to 87.0%. The removal rate is calculated as shown in Eq. 1.

Feng et al. (2018) employed sodium thiosulfate to enhance the degradation of methoxybenzamidine by potassium ferrate, indicating that the oxidation of methoxybenzamidine is attributed to the reaction between Fe (VI) and the reducing agent, generating intermediate states of Fe (IV) and Fe (V), thereby enhancing the oxidative capability of the potassium ferrate system. Similarly, Zhao et al. (2023) utilized sulfite to enhance the removal of polycyclic aromatic hydrocarbons by K2FeO4, confirming that the key active species involved in the degradation of polycyclic aromatic hydrocarbons are Fe (V) and Fe (IV). Because nZVI is a reducing agent, it generates Fe^{5+} and Fe^{4+} from K_2FeO_4 with stronger oxidizing ability by electron transfer. However, when the nZVI dosing concentration was greater than 100 mg/L, too much nZVI reduced Fe^{6+} to Fe^{5+} and Fe^{4+} and then continued to participate in the reaction, resulting in the consumption of a large amount of K_2FeO_4, intermediate valence iron with the reduction reaction of nZVI, and at the same time, too much intermediate valence iron will also be self-decomposed to generate Fe^{2+} and Fe^{3+} due to the lower stability and reduce the removal of two kinds of organotin (Oh et al., 2010). In the degradation removal of TPhT, more intermediate valence state iron was further generated to enhance the removal of TPhT due to the control of nZVI dosing and the increase of K_2FeO_4 dosing (Feng et al., 2018). However, the rate of intermediate valence state

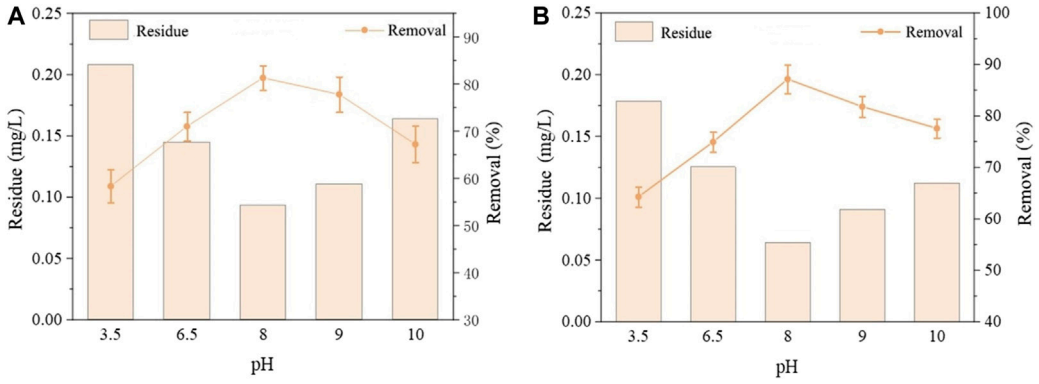

FIGURE 2
The influence of initial solution pH on the removal of TBT **(A)** and TPhT **(B)**.

iron produced by nZVI and K_2FeO_4 was accelerated when the dosing ratio was too large, which led to increased consumption of intermediate valence state iron due to its degradation, resulting in a decrease in the reaction rate. Meanwhile, the stability of K_2FeO_4 decreased due to higher concentration, and the hydrolysis into Fe^{2+} and Fe^{3+} also promoted the further decomposition of K_2FeO_4, leading to a decrease in the effective K_2FeO_4 concentration for oxidizing TPhT. Based on the double electron transfer mechanism, the previous authors proposed that there would be H_2O_2 generation in the hydrolysis of high valence iron species, and the process is the same as the reaction between nZVI and pertechnetate, which is exothermic, so that the self-decomposition of appropriate amount of K_2FeO_4 would promote the degradation of pollutants by other reactions (Jiang et al., 2016). Guo et al. (2013) found that the removal of heavy metals in water through the coupling of oxidizers and nZVI. The solubility of the oxidizer in water was higher than that of oxygen, which promoted diffusion on liquid/solid surfaces and high stability reactions on the nZVI surface, generating a large number of micrometer- or nanoscale colloids, which enhanced the removal of TBT and TPhT by adsorption and precipitation.

3.2 Effect of pH on the removal of organotin by nZVI and K_2FeO_4

As calculated based on Figures 2A, B, and Eq. 1; it can be seen that the removal rate of the two organotin species increased with pH, and the overall trend was first increasing and then decreasing. At pH 8.0, the removal rate of TBT and TPhT reached a maximum of 81.6% and 87.3%, respectively. pH is an important factor affecting water treatment, different pH conditions not only change the ionic form of K_2FeO_4 in the water body, but also change the redox potential and stability and thus affect the oxidation activity. Under acidic conditions K_2FeO_4 mainly exists in the form of protonation, respectively, $H_3FeO_4^+$, H_2FeO_4, $HFeO_4^-$, which with the proton attached to the oxygen of FeO_4^{2-} ions, so that the $HFeO_4^-$ has a higher spin density and thus oxidizing ability to be enhanced, to play a better oxidizing effect (Jiang, 2007; Yang et al., 2019; Hu, 2021); however, too low a pH will lead to the high potassium iron oxalate stability and reduce the removal of the two organotins. Under alkaline conditions, K_2FeO_4 exists mainly in the form of FeO_4^{2-}, and the lower spin density leads to a decrease in oxidizing ability; at the same time, the redox potential of K_2FeO_4 gradually decreases from +2.2 V under acidic conditions to +0.72 V under alkaline conditions, and the stability is greatly enhanced, although the oxidizing property is weakened (Jiang, 2007; Du et al., 2021). Therefore, at pH 8, the contact time of K_2FeO_4 with TBT and TPhT was prolonged and it also retained its oxidizing ability to TBT and TPhT with the best removal effect. In addition, under alkaline conditions, the surface of nZVI is negatively charged and K_2FeO_4 exists mainly in the form of negatively charged FeO_4^{2-} ions (Dong et al., 2016). Therefore, at pH 8, nZVI with a lower negative charge was able to slow down the reduction of K_2FeO_4 and increase the utilization of K_2FeO_4. However, as the pH continues to increase so that the repulsive reaction between the two is enhanced, the intermediate valence state of iron produced by the interaction of nZVI with K_2FeO_4 shifts from slowing to inhibiting, thus reducing the degradation of TBT and TPhT.

3.3 Reaction kinetics of nZVI and K_2FeO_4 for the removal of organotin

It can be seen that the overall degradation trends of TBT and TPhT were consistent and increasing with the reaction time (Figures 3A, B). The removal of TBT and TPhT degraded the fastest in 0–50 min, the degradation rates of TBT and TPhT slowed down in 50–80 min, and the concentrations of both stabilized after 100 min. In addition, the overall degradation reaction rate constants of TBT and TPhT also increased with the increase of the K_2FeO_4 and nZVI dosing ratio, and reached the maximum at dosing ratios of 1:1 and 3:1, respectively, which were 0.0162 s^{-1} and 0.0203 s^{-1}, respectively.

In the nZVI-enhanced degradation of TBT and TPhT by K_2FeO_4, the sole introduction of nZVI failed to elicit any discernible influence on the degradation process. Consequently, it can be deduced that K_2FeO_4 remained the principal oxidizing agent. Under typical conditions, when two reactants partake in a reaction, if the stoichiometries of the two compounds are

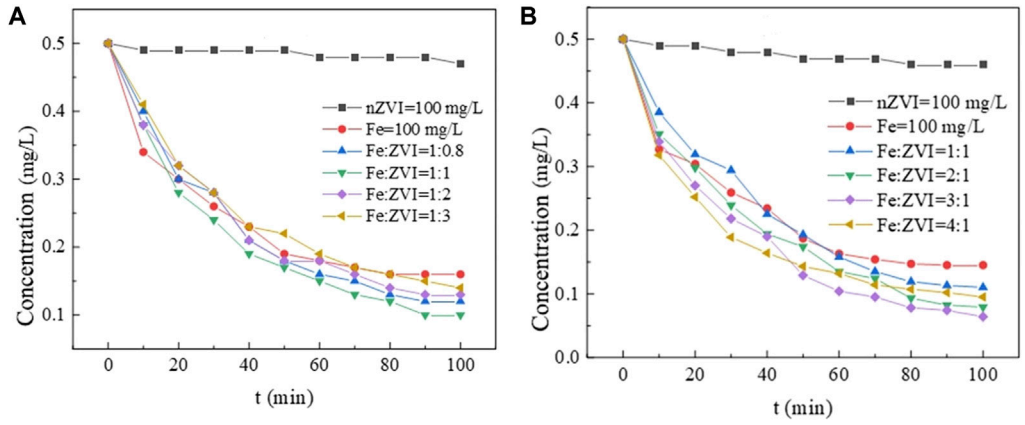

FIGURE 3
The impact of reaction time on the removal of TBT **(A)** and TPhT **(B)**.

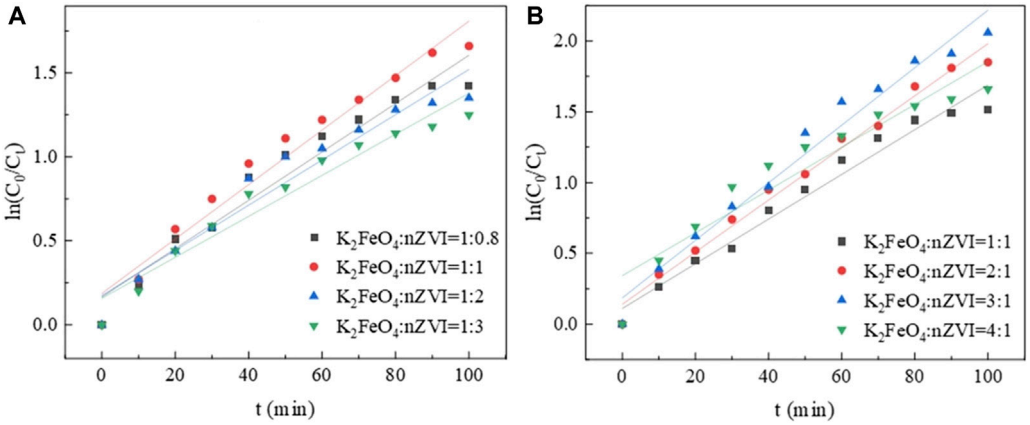

FIGURE 4
Effect of Reaction Time on ln (C_0/C_t) in the Removal of TBT **(A)** and TPhT **(B)**.

TABLE 1 The reaction rate equation and rate constant of TBT removal with different dosing ratios.

Order number	Dosing ratio of K_2FeO_4 to nZVI	Linear equation	K	R^2
1	1:0	ln (C_0/C) = 0.0146t + 0.1733	0.0146	0.9355
2	1:0.8	ln (C_0/C) = 0.0143t + 0.1659	0.0143	0.9509
3	1:1	ln (C_0/C) = 0.0162t + 0.1863	0.0162	0.9648
4	1:2	ln (C_0/C) = 0.0134t + 0.1740	0.0134	0.9429
5	1:3	ln (C_0/C) = 0.0122t + 0.1577	0.0122	0.9471

comparable and the concentrations differ by more than one order of magnitude, it may be inferred that the concentration of the higher-concentration substance remains consistent throughout the entirety of the reaction. Thus, the secondary reaction rate equation can be transmuted into a primary reaction rate equation. The reaction of K_2FeO_4 with TBT or TPhT belongs to the secondary reaction, but the amount of K_2FeO_4 dosed in the present experiment is one order of magnitude greater than that of TBT or TPhT, so the K_2FeO_4 in the experiment is regarded as a constant, and the oxidative degradation is inferred to follow the quasi-primary reaction kinetics. Data fitting was performed according to Eq. 3, and the equation of ln (C_0/C_t) versus time for TBT and TPhT at different K_2FeO_4 dosages is shown in Figures 4A, B. As can be seen from Tables 1, 2, the linear coefficients of both TBT and TPhT in the fitted straight line are greater than 0.9, which has a good linear relationship.

TABLE 2 The reaction rate equation and rate constant of TPhT removal with different dosing ratios.

Order number	Dosing ratio of K_2FeO_4 to nZVI	Linear equation	K	R^2
1	1:0	ln (C_0/C) = 0.0158t + 0.1491	0.0158	0.9570
2	1:1	ln (C_0/C) = 0.0157t + 0.1109	0.0157	0.9718
3	2:1	ln (C_0/C) = 0.0184t + 0.1404	0.0184	0.9854
4	3:1	ln (C_0/C) = 0.0203t + 0.1854	0.0203	0.9727
5	4:1	ln (C_0/C) = 0.0151t + 0.3418	0.0151	0.9038

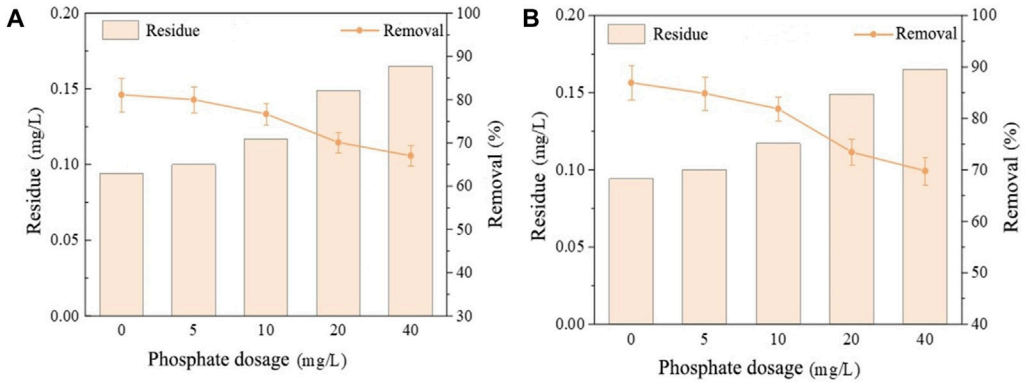

FIGURE 5
Influence of carbonate dosage on the removal effect of TBT **(A)** and TPhT **(B)**.

3.4 Effect of nZVI and K_2FeO_4 on organotin removal in simulated real waters

Generally, the actual water body contains more impurity components, and their presence has a certain effect on the treatment of TBT and TPhT (Dong, 2009). Therefore, carbonate and humic acid, which are common in actual water bodies, were chosen to simulate actual water bodies and explore the reaction effect in simulated actual water bodies. As calculated based on Figures 5A, B, and Eq. 1; carbonate inhibits the degradation and removal of TBT and TPhT, and the inhibition increases with the increase of carbonate concentration. The degradation rate of TBT decreased from 81.6% to 67.1% and that of TPhT decreased from 87.0% to 69.8% when the carbonate dosing in the solution increased from 0 mg/L to 40 mg/L. The degradation rate of TBT decreased from 81.6% to 67.1% and that of TPhT decreased from 87.0% to 69.8%. Carbonate ions (CO_3^{2-}) affected the removal of both organotins due to their own hydrolysis; meanwhile, CO_3^{2-} interacted with Fe $(OH)_3$ generated by the redox of K_2FeO_4 to generate inner-sphere chelating ligand compounds, which led to an increase in the pH of the solution and altered the degradation of TBT and TPhT by K_2FeO_4 (Jain et al., 2009). In addition, based on the effect of tert-butanol on the degradation of TBT and TPhT in Section 2.5, it can be seen that the generated hydroxyl radical (OH) is involved in the degradation of organotin, and Buxton et al. (1988) found by determining the rate of the secondary reaction between CO_3^{2-} and OH that CO_3^{2-} was able to effectively burst the OH through the following reaction process, which further affected the degradation of TBT and TPhT. The related chemical reactions are shown in Eqs. 4–6;

$$\boldsymbol{CO_3^{2-} + \cdot OH \rightarrow \cdot CO_3^{-} + OH^{-}} \quad (4)$$

$$\boldsymbol{HCO_3^{-} + \cdot OH \leftrightarrow \cdot CO_3^{-} + H_2O} \quad (5)$$

$$\boldsymbol{\equiv Fe\text{-}OH + CO_3^{2-} \rightarrow \equiv Fe\text{-}O\text{-}CO_2^{-} + OH^{-}} \quad (6)$$

Humic acid belongs to macromolecular organic compounds, which widely exist in various natural water environments; among them, xanthate is the main component of organic matter in natural water environments due to its ability to dissolve in water (Jin et al., 2020), therefore, xanthate was chosen to explore the influence of the effect on the removal of TBT and TPhT. According to Jiang and Wang (2003) the utilization of K_2FeO_4 for degrading and removing UV_{254} absorbance, dissolved organic carbon, and reducing the formation potential of trihalomethanes is noteworthy. It is evident that at a pH of 7.8 and a humic acid concentration of 10 mg/L, the addition of 0.04–0.82 mM of Fe (VI) can result in a reduction in UV_{254} by 21%–74%. As calculated based on Figures 6A, B, and Eq. 1; it can be seen that the addition of xanthate produced a strong inhibitory effect on the removal rate of degraded TBT and TPhT compared to no xanthate addition, and the inhibitory effect increased with the increase of the concentration of xanthate addition. When the concentration of xanthate was increased from 5 mg/L to 40 mg/L, the removal rates of TBT and TPhT decreased from 75.5% to 82.4%–37.6% and 46.7%, respectively. Xanthic acid inhibited the removal of organotin mainly

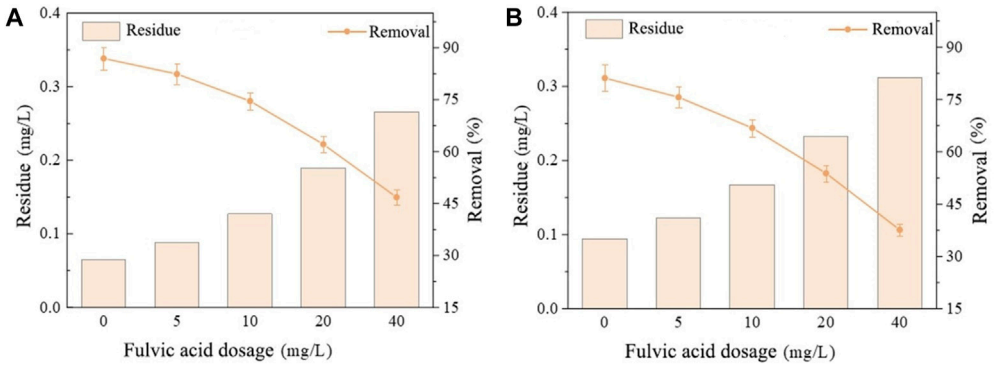

FIGURE 6
Effect of xanthate dosing concentration on the removal of TBT **(A)** and TPhT **(B)**.

because it belongs to the aromatic compounds itself and competes with TBT and TPhT for the reaction of K_2FeO_4 through phenolic hydroxyl and other groups, while consuming the intermediate valence iron and hydroxyl groups produced, thus decreasing the removal efficacy of TBT and TPhT. In addition, Fe^{2+} generated from the oxidative decomposition of K_2FeO_4 is also consumed by xanthic acid, which reduces the reaction of Fe^{2+} to promote the generation of intermediate valence iron from K_2FeO_4, leading to a further decrease in the degradation efficacy for TBT and TPhT.

3.5 Mechanistic study of organotin degradation by nZVI and K_2FeO_4

3.5.1 The role of OH

TBA was a typical free radical inhibitor, which can consume a large amount of OH produced by the decomposition of K_2FeO_4 and interrupt the chain reaction of free radicals (Lindsey M E, 2000). TBA reacts with OH at a reaction rate of 6×10^8 mol $(L{\cdot}s)^{-1}$, which can rapidly react with OH to achieve the removal of OH, and related studies have shown that the effect of OH can also effectively degrade organotin (Zhang et al., 2021). Therefore, the selection of TBA as a radical scavenger aims to investigate the generation of OH and its impact on the removal of two organic tin species. As calculated based on Figures 7A, B, and Eq. 1; it can be seen that the addition of TBA inhibitor inhibited the removal of both organotin species, and the inhibition of TBT and TPhT was the greatest when the concentration of TBA dosing was 1 mg/L, which decreased by 42.6% and 35.6%, respectively. The inhibition of the degradation of TBT and TPhT was gradually weakened when the TBA dosing concentration continued to increase. nZVI-enhanced K_2FeO_4 had the generation of OH in addition to the intermediate valence state of iron produced, which contributed to the removal of TBT and TPhT. It was also shown that K_2FeO_4 in solution was reduced by organic radicals (ROH, where ROH = methanol, ethanol, isopropanol, or tert-butanol) to generate Fe^{5+}, and because these radicals have certain diffusion-controlled rate constants, when TBA was added, it rapidly reacted with OH to generate simple carbon-centered radicals through the reaction and thus reduced Fe^{6+} through diffusion-controlled rate constants to generate Fe^{5+} (Sun et al., 2018). Therefore, the excessive addition of TBA favors the generation of Fe^{5+} from K_2FeO_4 and weakens the inhibition of the degradation of TBT and TPhT.

3.5.2 Theoretical calculation

As a supplement to the experimental work, theoretical calculations have been applied to reveal the transformation mechanism of various organic pollutants (Cao et al., 2021; Qi et al., 2021). According to Figures 8A–E, compared with triphenyltin, in the presence of Fe (IV) and Fe (V), the Sn-C bond length becomes longer, and the longer the bond length, the easier it is to break the bond, indicating that the more unstable, and the generated OH is more likely to attack the benzene ring (Mahmoudi et al., 2020). In addition, according to Wang et al. (2023), the interaction between Fe (VI), carbon quantum dots (CQDs) and phenol was revealed by theoretical calculation. It can be seen that the values of HOMO and LUMO reflect the ability of molecules to lose and accept electrons. The higher the HOMO orbital energy is, the more unstable the electrons in the orbit are, and the easier it is to lose electrons and be oxidized. The lower the LUMO orbital energy, the easier it is to accept electrons and be reduced. According to Figures 9A–C, in the presence of Fe (IV) and Fe (V), the HOMO energy level increases, and it is easier to lose electrons, and $(C_6H_5)_3Sn^+$ -Fe (V) is the largest, −3.36 eV; therefore, Fe (V) is more likely to oxidize triphenyltin.

The Gibbs free energy is calculated by DFT to evaluate the possibility of its occurrence and identify the main reaction channels (Figure 10) (Cao et al., 2021). According to the empirical rule, the reaction with an energy barrier of 21 kcal/mol or lower will proceed rapidly at room temperature (Qi et al., 2021). Therefore, although the Gibbs free energy of some reactions in Figure 10 is positive, the reaction can still proceed. Firstly, triphenyltin chloride is ionized in aqueous solution in the form of $(C_6H_5)_3Sn^+$ ions, and the ionization needs to overcome the energy barrier of 4.55 eV. Secondly, compared with the self-decomposition of $(C_6H_5)_3Sn^+$ and the presence of oxidizing active species, the energy barrier to overcome the gradual transformation of $(C_6H_5)_3Sn^+$ into Sn^{4+} gradually increases, while the energy barrier to overcome the transformation in the presence of Fe (IV) and Fe (V) gradually decreases, indicating that it is easier to break bonds in the presence of Fe (IV) and Fe (V), and finally oxidize to inorganic tin ions. In

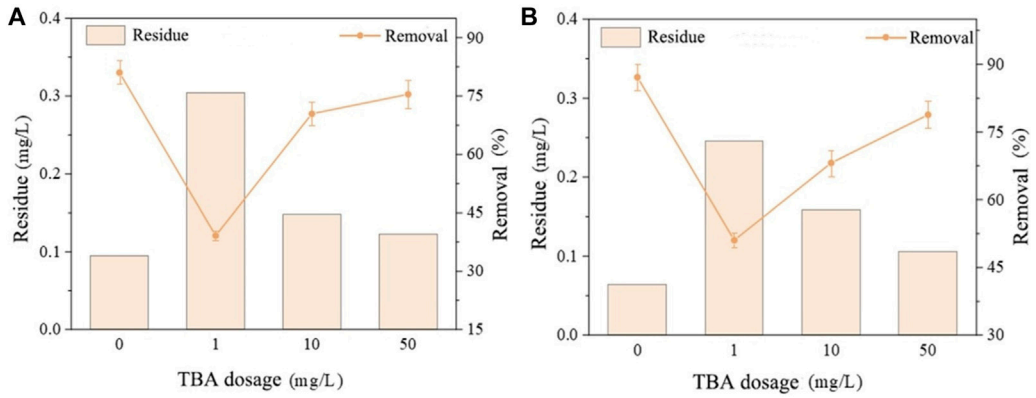

FIGURE 7
Effect of different TBA concentrations on the removal of TBT **(A)** and TPhT **(B)**.

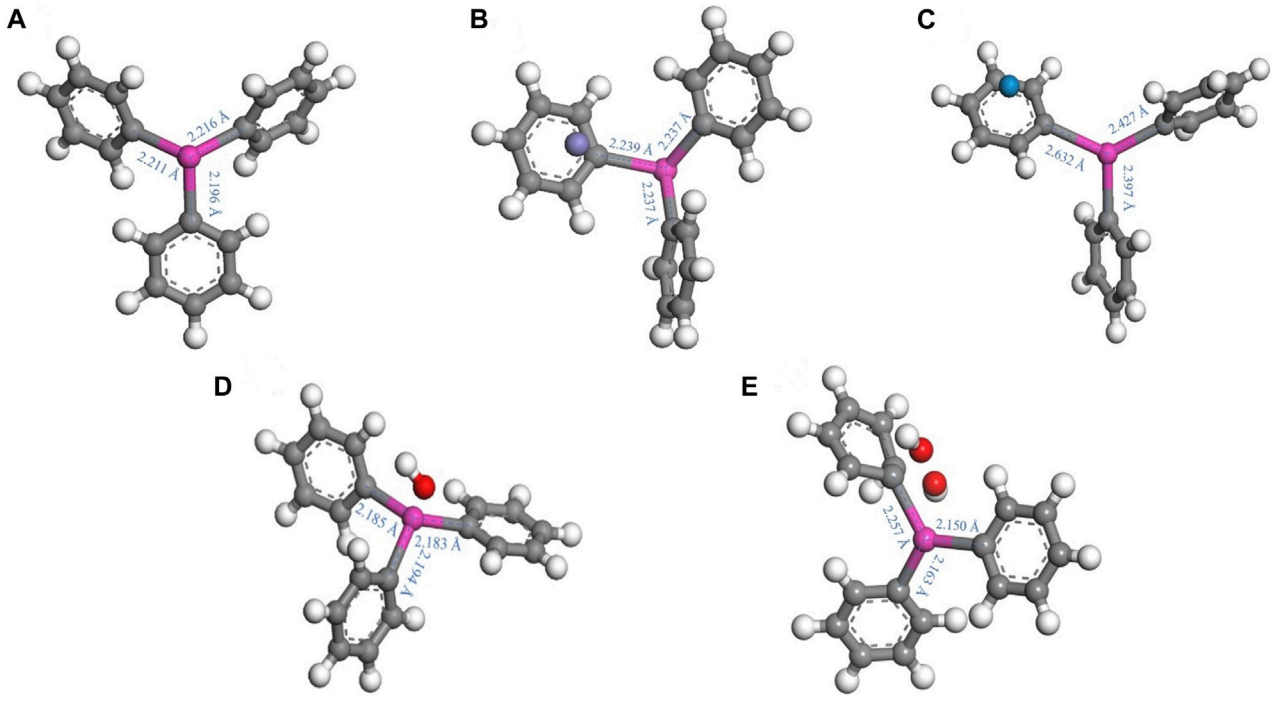

FIGURE 8
Structural diagrams and changes in bond lengths of triphenyltin in different states; **(A)** $(C_6H_5)_3$ Sn^+; **(B)** $(C_6H_5)_3$ Sn^+—Fe (IV); **(C)** $(C_6H_5)_3$ Sn^+—Fe (V); **(D)** $(C_6H_5)_3$ Sn^+—OH; **(E)** $(C_6H_5)_3$ Sn^+—2·OH. [Atomic colours: white, hydrogen; grey, carbon; pink, tin; red, oxygen; purple, Fe (IV); blue, Fe (V)].

addition, it can be seen from Figures 11A, B that in the presence of Fe (IV) and Fe (V), the Sn-C bond in diphenyltin is too long, resulting in the direct cleavage of the bond. Therefore, diphenyltin could not exist stably under these conditions, and it also verified why the relevant intermediate products could not be detected by GC-MS. Finally, nZVI enhances the production of OH in K_2FeO_4, and the reaction energy barrier gradually decreases. It is necessary to overcome the lower energy and is easier to degrade triphenyltin. Therefore, OH plays a more critical role in the removal of triphenyltin, which is consistent with the inhibition experimental results.

3.5.3 The mechanism by which nZVI enhances the degradation of TBT and TPhT by K_2FeO_4

$$(Ph)_3SnCl + H_2O \leftrightarrow (Ph)_3Sn^+ + Cl^- \quad (7)$$

$$(Ph)_3Sn^+ + \cdot OH \rightarrow [(Ph)_3Sn(OH)]^{+\cdot} \quad (8)$$

$$[(Ph)_3Sn(OH)]^{+\cdot} \rightarrow (Ph)_3Sn^+ + \cdot OH \quad (9)$$

$$[(Ph)_3Sn(OH)]^{+\cdot} \rightarrow Ph^{\cdot} + [(Ph)_2Sn(OH)]^+ \quad (10)$$

To further understand the reaction path of nZVI-enhanced K_2FeO_4 degradation of TBT and TPhT, combined with the

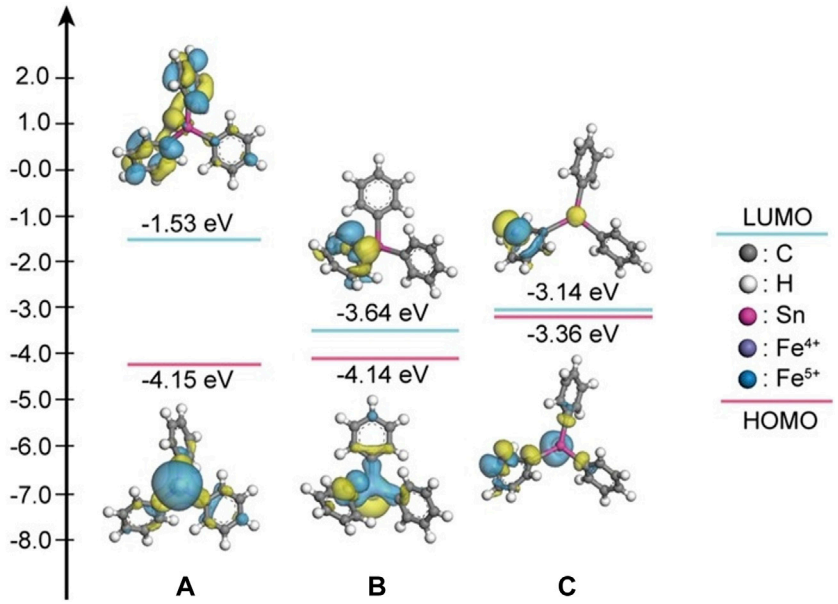

FIGURE 9
LUMO and HOMO energy level diagrams; **(A)** $(C_6H_5)_3$ Sn^+; **(B)** $(C_6H_5)_3$ Sn^+—Fe (IV); **(C)** $(C_6H_5)_3$ Sn^+—Fe (V).

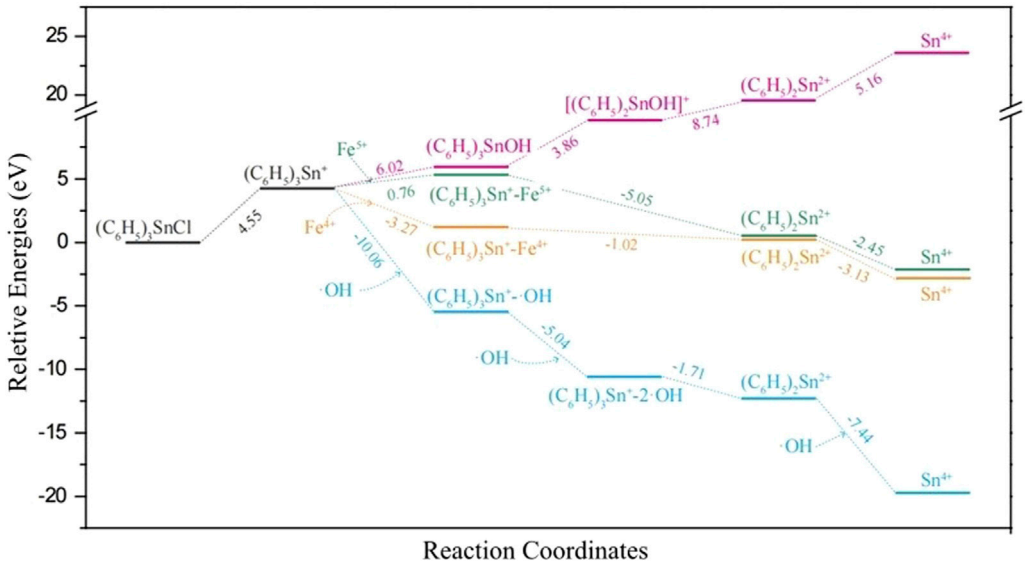

FIGURE 10
Gibbs free energy diagram of organotin degradation by nZVI-enhanced K_2FeO_4.

previous degradation experiments and theoretical calculations, the intermediate products of TBT in the degradation process were qualitatively detected. The test results are shown in Table 3. Ferrate has strong oxidizing and electrophilic properties, and nZVI enhances K_2FeO_4 to produce high oxidizing intermediate valence Fe^{4+} and Fe^{5+} (Li et al., 2018; Zhao et al., 2018). Combined with TBA experiments, it can be seen that nZVI reduces K_2FeO_4 to produce OH. Since the redox potential of OH is 2.8 V (Psaltou et al., 2019), using the classical argument of organic chemistry, the adjacent carbon atoms of the tin atom should be partially negatively charged, thereby increasing the rate constant of the electrophilic OH reaction. In chemical degradation, Sn-C cleavage occurs through nucleophilic or electrophilic attacks such as inorganic acids and alkali metals (Hoch, 2001) to remove organotin pollutants. The intermediate oxidation products of TBT were detected by GC-MS. It was found that mono butyl derivative tin and dibutyl derivative tin appeared in the degradation products of TBT, which proved that ferrate and

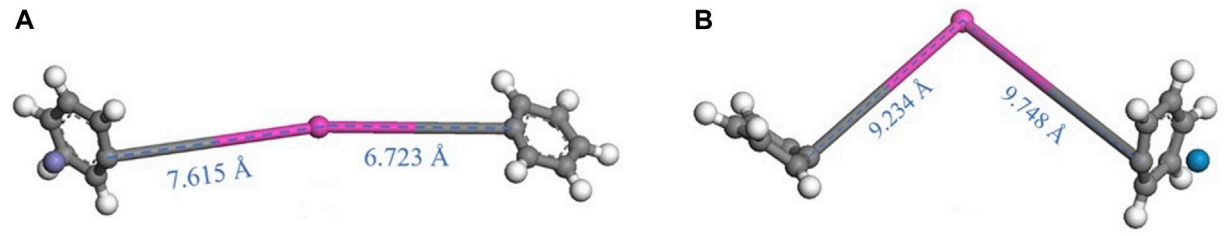

FIGURE 11
Structure of diphenyltin: **(A)** $(C_6H_5)_2$ Sn^{2+}—Fe (IV); **(B)** $(C_6H_5)_2$ Sn^{2+}—Fe (V); [Atomic colours: white, hydrogen; grey, carbon; pink, tin; red, oxygen; violet, Fe (IV); blue, Fe (V)].

TABLE 3 Intermediate products detected in the degradation of TBT by GC-MS.

Chemical compound	CAS number	Molecular formula	Molecular weight	Structure
Dibutylstannane	1002-53-5	$C_8H_{20}Sn$	236	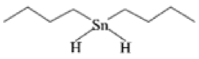
ButyltrimethylStannane	1527-99-7	$C_7H_{18}Sn$	222	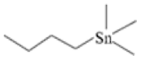

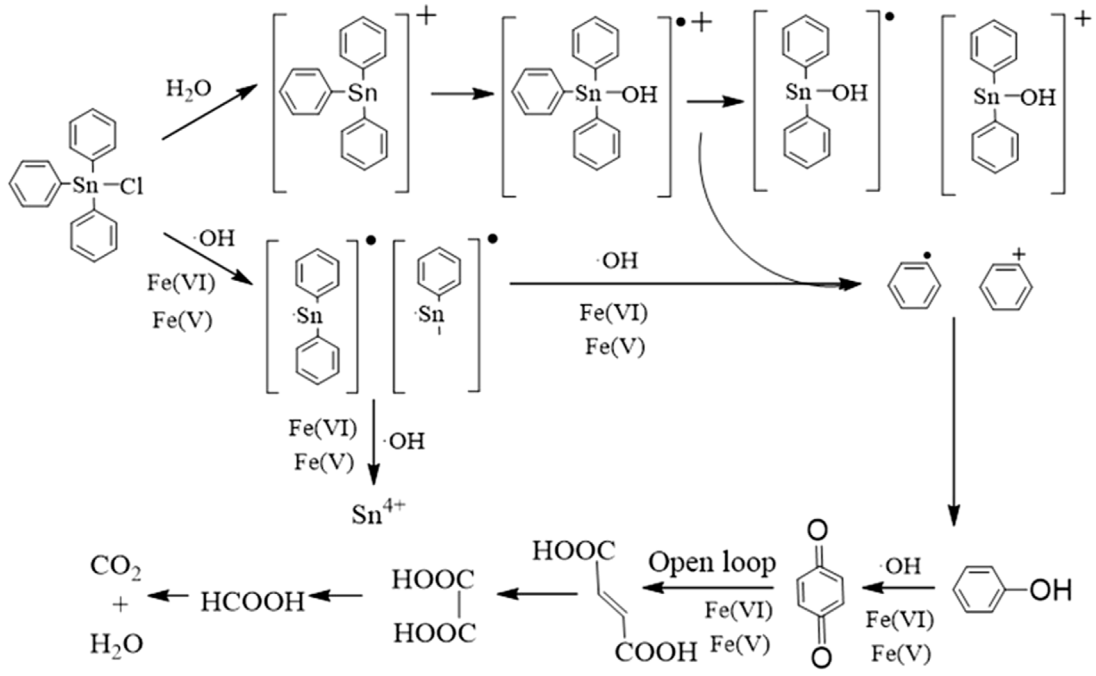

FIGURE 12
Mechanistic diagram of organotin degradation by K_2FeO_4 and nZVI.

OH broke Sn-C by the electrophilic attack, and then removed butyl from TBT, confirming that the process of oxidative degradation of TBT was a process of deacetylation. Inorganic tin ions were not detected in the final degradation products, because a variety of strong oxidizing ions produced by nZVI-enhanced K_2FeO_4 oxidized Sn^{2+} to Sn^{4+}, and Sn^{4+} was usually precipitated in the form of Sn $(OH)_4$ under alkaline conditions, which explained the reason why inorganic tin ions were not detected. Similar to the process of TBT deacetylation, the degradation of TPhT is a dephenylation process and is eventually oxidized to inorganic tin ions. However, the intermediate derivatives of tin were not detected by GC-MS. According to theoretical calculations, diphenyltin was directly broken because the Sn-C bond was too long. In addition to the

process of oxidative cleavage of Sn-C and phenyl removal by oxidizing active species, CAO et al. (2008) found that TPhT interacts with water in water to cause Sn-Cl cleavage to form $(Ph)_3Sn^+$. In addition, the generated OH can also attack the benzene ring on the cation of $(Ph)_3Sn^+$ to generate $[(Ph)_2Sn(OH)]^+$. Since $[(Ph)_2Sn(OH)]^+$ is transient and unstable, it can generate $(Ph)_3Sn^+$, $[(Ph)_2Sn(OH)]^+$, $(Ph)_2Sn^{\cdot}(OH)$, $Ph^{\cdot}$ and Ph^+ ions through self-decomposition to achieve dephenylation of TPhT. The relevant chemical reactions are shown in Eqs. 7–10.

In addition, Deng et al. (2009) found that phenyl radicals generate phenol with water by GC-MS analysis of degraded phenol products. Since phenol is reactive, the oxidizing ions Fe^{6+}, Fe^{5+}, Fe^{4+}, and OH at this time will further oxidize it to substances such as phenyldiphenol, benzoquinone and phenoxyphenol. With the gradual increase in the dosage of K_2FeO_4 and nZVI, enough oxidizing ions are generated to perform the ring-opening reaction on the benzene ring to ultimately produce substances such as maleic acid and oxalic acid (Zhang et al., 2013). Combining the above factors, it is inferred that the degradation reaction of TPhT is shown in Figure 12.

4 Conclusion

This study aims to enhance the removal efficiency of TBT and TPhT by employing nZVI in conjunction with K_2FeO_4. The research findings indicate that, at a pH of 8, with K_2FeO_4 to nZVI dosage ratios of 1:1 and 3:1, the degradation removal rates for TBT and TPhT are 81.6% and 87.0%, respectively, with corresponding rate constants of 0.0162 and 0.0203. The variation in pH not only influences the oxidative capacity and stability of K_2FeO_4 but also alters the surface charge of nZVI, thereby attenuating its reducing effect on K_2FeO_4. Additionally, in simulated natural water bodies, carbonate undergoes self-hydrolysis, altering pH and consuming OH. Simultaneously, phenolic hydroxyl groups in humic acid consume intermediate state iron and OH, thereby diminishing the efficiency of TBT and TPhT removal. Through GC-MS detection and chemical calculations, it is observed that TBT's intermediate degradation products include monobutyl and dibutyl derivatives of tin, while in TPhT, the Sn-C bond length increases, HOMO energy level rises, and the overcoming barrier gradually decreases. This indicates that the intermediate iron state and OH generated by nZVI enhance K_2FeO_4 progressively attack the Sn-C bonds in TBT and TPhT, gradually de-alkylating or de-phenylating, and ultimately oxidizing them into inorganic tin ions. Furthermore, the generated OH may form compounds through hydrolysis with TPhT, facilitating the removal of phenyl groups through hydrolysis. The study results reveal the degradation efficiency and pathways of two organic tin compounds using the nZVI-enhanced K_2FeO_4 method. This approach demonstrates the ability to rapidly degrade organic tin and is not restricted in most application scenarios, thereby reducing the secondary pollution of water bodies. This method provides valuable insights for the degradation of water bodies contaminated with organic tin in channels, ports, lakes, and similar environments. In future experimental studies, incorporating tests for intermediate valence iron can further elucidate the mechanism of organic tin removal.

Data availability statement

The original contributions presented in the study are included in the article/Supplementary material, further inquiries can be directed to the corresponding authors.

Author contributions

YH: Conceptualization, Data curation, Formal Analysis, Investigation, Visualization, Writing–original draft, Writing–review and editing. QY: Conceptualization, Data curation, Formal Analysis, Investigation, Methodology, Validation, Visualization, Writing–original draft, Writing–review and editing. LS: Data curation, Funding acquisition, Investigation, Project administration, Writing–original draft. HR: Data curation, Formal Analysis, Writing–original draft. HJ: Conceptualization, Data curation, Formal Analysis, Investigation, Methodology, Visualization, Writing–original draft, Writing–review and editing. DS: Funding acquisition, Project administration, Resources, Supervision, Writing–original draft, Writing–review and editing.

Funding

The author(s) declare that financial support was received for the research, authorship, and/or publication of this article. This work was supported by The Ministry of Water Resources of China, the major scientific and technical project (SKS-2022076); Chongqing Technological Innovation and Application Development Special Key Project (CSTB2022TIAD-KPX0133); Chongqing Water Conservancy Science and Technology Project (CQSLK-2022001); Chongqing Technology Foresight and System Innovation Project (CSTB2023TFII-OIX0022); Chongqing 2023 Urban Management Scientific Science Project (CGKZ2023-16); Chongqing Science and Technology Innovation Key Project for Social Undertakings and People's Livelihood Security (CSTC2017shms-zdyfX0028).

Conflict of interest

Author LS was employed by Chongqing Water Group Co., Ltd.

The remaining authors declare that the research was conducted in the absence of any commercial or financial relationships that could be construed as a potential conflict of interest.

Publisher's note

References

Bouakline, H., Elkabous, M., Ziani, I., Karzazi, Y., Tahani, A., and El Bachiri, A. (2023). Antioxidative activity of Pistacia lentiscus leaf extract main components: experimental and theoretical study. *Mater. Today Proc.* 72, 3275–3279. doi:10.1016/j.matpr.2022.07.241

Brosillon, S., Bancon-Montigny, C., and Mendret, J. (2014). Study of photocatalytic degradation of tributyltin, dibutylin and monobutyltin in water and marine sediments. *Chemosphere* 109, 173–179. doi:10.1016/j.chemosphere.2014.02.008

Buxton, G. V., Greenstock, C. L., Phillips, H. W., Ross, A. B., and Tsang, W. (1988). Critical Review of rate constants for reactions of hydrated electrons, hydrogen atoms and hydroxyl radicals·OH/·O^- in Aqueous Solution. *J. Phys. Chem. reference data* 17, 513–886. doi:10.1063/1.555805

Cao, C. Q., Huang, L., Zhang, R. X., Dong, W. B., and Hou, H. Q. (2008). Study on the reaction mechanism of triphenyltin with ·OH radical in aqueous phase by transient absorbance spectra. *ACTA CHIM. SIN.* 01, 112–116. doi:10.3321/j.issn:0567-7351.2008.01.019

Cao, H., Han, D., Li, M., Li, X., He, M., and Wang, W. (2015). Theoretical investigation on mechanistic and kinetic transformation of 2,2',4,4',5-pentabromodiphenyl ether. *J. Phys. Chem. A* 119 (24), 6404–6411. doi:10.1021/acs.jpca.5b04022

Cao, W., Wu, N., Qu, R., Sun, C., Huo, Z., Ajarem, J. S., et al. (2021). Oxidation of benzophenone-3 in aqueous solution by potassium permanganate: kinetics, degradation products, reaction pathways, and toxicity assessment. *Environ. Sci. Pollut. Res. Int.* 28 (24), 31301–31311. doi:10.1007/s11356-021-12913-x

Chang, E.-E., Chang, Y.-C., Liang, C.-H., Huang, C.-P., and Chiang, P.-C. (2012a). Identifying the rejection mechanism for nanofiltration membranes fouled by humic acid and calcium ions exemplified by acetaminophen, sulfamethoxazole, and triclosan. *J. Hazard. Mater.* 221, 19–27. doi:10.1016/j.jhazmat.2012.03.051

Chang, E. E., Chang, Y. C., Liang, C. H., Huang, C. P., and Chiang, P. C. (2012b). Identifying the rejection mechanism for nanofiltration membranes fouled by humic acid and calcium ions exemplified by acetaminophen, sulfamethoxazole, and triclosan. *J. Hazard Mater* 221-222, 19–27. doi:10.1016/j.jhazmat.2012.03.051

Chen, C., Chen, L., Huang, Q., Chen, Z., and Zhang, W. (2019). Organotin contamination in commercial and wild oysters from China: increasing occurrence of triphenyltin. *Sci. Total Environ.* 650 (Pt 2), 2527–2534. doi:10.1016/j.scitotenv.2018.09.310

Chen, G. (2012). *Experimental study on the treatment of organophosphorus pesticide wastewater by UV/ferrate*. Master. Huazhong University Of Science And Technology.

Chen, X. (2019). *Multi-media fate simulation and risk assessment of organotin in water environment under dynamic water level in the Three Gorges Reservoir area*. Master. Chongqing University.

De Carvalho Oliveira, R., and Santelli, R. E. (2010). Occurrence and chemical speciation analysis of organotin compounds in the environment: a review. *Talanta* 82 (1), 9–24. doi:10.1016/j.talanta.2010.04.046

Deng, Z., Yang, X., and Xu, W. (2009). GC-MS analysis of phenol degradation by potassium ferrate. *J. Tongji Univ. Nat. Sci. Ed.* 37 (03), 354–357.

Dong, H., Ahmad, K., Zeng, G., Li, Z., Chen, G., He, Q., et al. (2016). Influence of fulvic acid on the colloidal stability and reactivity of nanoscale zero-valent iron. *Environ. Pollut.* 211, 363–369. doi:10.1016/j.envpol.2016.01.017

Dong, J. (2009). *Study on oxidative degradation of bisphenol A in water by potassium ferrate*. Master. Hunan University.

Du, J., Chadalavada, S., Chen, Z., and Naidu, R. (2014). Environmental remediation techniques of tributyltin contamination in soil and water: a review. *Chem. Eng. J.* 235, 141–150. doi:10.1016/j.cej.2013.09.044

Du, Y., Gao, P., Yang, J., Shi, F., and Shabaz, M. (2021). Experimental Analysis of mechanical properties and durability of cement-based composite with carbon nanotube. *Adv. Mater. Sci. Eng.* 2021, 1–12. doi:10.1155/2021/8777613

Feng, M., Jinadatha, C., Mcdonald, T. J., and Sharma, V. K. (2018). Accelerated oxidation of organic contaminants by ferrate (VI): the overlooked role of reducing additives. *Environ. Sci. Technol.* 52 (19), 11319–11327. doi:10.1021/acs.est.8b03770

Fent, K. (1996). Ecotoxicology of organotin compounds. *Crit. Rev. Toxicol.* 26, 3–117. doi:10.3109/10408449609089891

Gao, J., Hu, J., Jin, X., An, L., and Zheng, Z. (2004). Investigation of organotin pollution in water environment China. *Water & amp* (07), 25–27. doi:10.3321/j.issn:1000-4602.2004.07.006

Guo, Y., Lou, X., Fang, C., Xiao, D., Wang, Z., and Liu, J. (2013). Novel photo-sulfite system: toward simultaneous transformations of inorganic and organic pollutants. *Environ. Sci. Technol.* 47 (19), 11174–11181. doi:10.1021/es403199p

Han, Q., Wang, H., Dong, W., Liu, T., and Yin, Y. (2013). Formation and inhibition of bromate during ferrate(VI)–Ozone oxidation process. *Sep. Purif. Technol.* 118, 653–658. doi:10.1016/j.seppur.2013.07.042

Hassan, H. A., Dawah, S. E., and El-Sheekh, M. M. (2019). Monitoring the degradation capability of novel haloalkaliphilic tributyltin chloride (TBTCl) resistant bacteria from butyltin-polluted site. *Rev. Argent. Microbiol.* 51 (1), 39–46. doi:10.1016/j.ram.2017.12.002

Hoch, M. (2001). Organotin compounds in the environment—an overview. *Appl. Geochem.* 16 (7-8), 719–743. doi:10.1016/s0883-2927(00)00067-6

Hu, H., Wang, H., Ying, Z., Sun, X., Li, T., Jin, Y., et al. (2020). Research progress on detection methods of organotin environmental hormones in environmental samples Journal of Zhejiang Ocean University. *Nat. Sci. Ed.* 39 (02), 156–162. doi:10.3969/j.issn.1008-830X.2020.02.010

Hu, Y. (2021). *Kinetics and mechanism of potassium ferrate oxidation of ebselen*. Master. Harbin Polytechnic Institute.

Jain, A., Sharma, V. K., and Mbuya, O. S. (2009). Removal of arsenite by Fe(VI), Fe(VI)/Fe(III), and Fe(VI)/Al(III) salts: effect of pH and anions. *J. Hazard Mater* 169 (1-3), 339–344. doi:10.1016/j.jhazmat.2009.03.101

Jiang, J. Q. (2007). Research progress in the use of ferrate(VI) for the environmental remediation. *J. Hazard Mater* 146 (3), 617–623. doi:10.1016/j.jhazmat.2007.04.075

Jiang, J.-Q., and Wang, S. (2003). Enhanced coagulation with potassium ferrate (VI) for removing humic substances. *Environ. Eng. Sci.* 20 (6), 627–633. doi:10.1089/109287503770736140

Jiang, Y., Goodwill, J. E., Tobiason, J. E., and Reckhow, D. A. (2016). Bromide oxidation by ferrate(VI): the formation of active bromine and bromate. *Water Res.* 96, 188–197. doi:10.1016/j.watres.2016.03.065

Jin, L., Yin, H., Tang, S., Yu, X., Yu, Y., and Liu, H. (2020). Degradation of tris (1,3-dichloroisopropyl-2-propyl) phosphate by UV activated persulfate water treatment technology. *U. S. Environ. Prot. Agency* 46 (10), 67–73. doi:10.16796/j.cnki.1000-3770.2020.10.014

Li, W., Yu, N., Liu, Q., Li, Y., Ren, N., and Xing, D. (2018). Enhancement of the sludge disintegration and nutrients release by a treatment with potassium ferrate combined with an ultrasonic process. *Sci. Total Environ.* 635, 699–704. doi:10.1016/j.scitotenv.2018.04.174

Li, Y., Jiang, L., Wang, R., Wu, P., Liu, J., Yang, S., et al. (2021). Kinetics and mechanisms of phenolic compounds by Ferrate(VI) assisted with density functional theory. *J. Hazard Mater* 415, 125563. doi:10.1016/j.jhazmat.2021.125563

Lindsey, M. E. T. M. A., and Tarr, M. A. (2000). Inhibition of hydroxyl radical reaction with aromatics by dissolved natural organic matter. *Environ. Sci. Technol.* 34, 444–449. doi:10.1021/es990457c

Liu, C., Han, M., Chen, C. L., Yin, J., Zhang, L., and Sun, J. (2023). Decorating phosphorus anode with SnO_2 nanoparticles to enhance polyphosphides chemisorption for high-performance lithium-ion batteries. *Nano Lett.* 23 (8), 3507–3515. doi:10.1021/acs.nanolett.3c00656

Liu, Y., Zhang, J., Huang, H., Huang, Z., Xu, C., Guo, G., et al. (2019). Treatment of trace thallium in contaminated source waters by ferrate pre-oxidation and poly aluminium chloride coagulation. *Sep. Purif. Technol.*, 227. doi:10.1016/j.seppur.2019.06.001

Mahmoudi, A., Shakibania, S., Rezaee, S., and Mokmeli, M. (2020). Effect of the chloride content of seawater on the copper solvent extraction using Acorga M5774 and LIX 984N extractants. *Sep. Purif. Technol.* 251, 117394. doi:10.1016/j.seppur.2020.117394

Oh, S. Y., Kang, S. G., and Chiu, P. C. (2010). Degradation of 2,4-dinitrotoluene by persulfate activated with zero-valent iron. *Sci. Total Environ.* 408 (16), 3464–3468. doi:10.1016/j.scitotenv.2010.04.032

Pagliarani, A., Nesci, S., and Ventrella, V. (2013). Toxicity of organotin compounds: shared and unshared biochemical targets and mechanisms in animal cells. *Toxicol Vitro* 27 (2), 978–990. doi:10.1016/j.tiv.2012.12.002

Psaltou, S., Karapatis, A., Mitrakas, M., and Zouboulis, A. (2019). The role of metal ions on p-CBA degradation by catalytic ozonation. *J. Environ. Chem. Eng.* 7 (5), 103324. doi:10.1016/j.jece.2019.103324

Qi, Y., Wei, J., Qu, R., Al-Basher, G., Pan, X., Dar, A. A., et al. (2021). Mixed oxidation of aqueous nonylphenol and triclosan by thermally activated persulfate: reaction kinetics and formation of co-oligomerization products. *Chem. Eng. J.* 403, 126396. doi:10.1016/j.cej.2020.126396

Ribas, R., Cazarolli, J. C., Da Silva, E. C., Meneghetti, M. R., Meneghetti, S. M. P., and Bento, F. M. (2020). Characterization of antimicrobial effect of organotin-based catalysts on diesel-biodiesel deteriogenic microorganisms. *Environ. Monit. Assess.* 192 (12), 802. doi:10.1007/s10661-020-08744-x

Sakultantimetha, A., Keenan, H. E., Beattie, T. K., Aspray, T. J., Bangkedphol, S., and Songsasen, A. (2010). Acceleration of tributyltin biodegradation by sediment microorganisms under optimized environmental conditions. *Int. Biodeterior. Biodegrad.* 64 (6), 467–473. doi:10.1016/j.ibiod.2010.05.007

Song, W., Guo, J., Yang, Q., and Cheng, G. (2020). Research progress on degradation of sludge organic pollutants. *Chem. Industry Eng. Prog.* 39 (01), 380–386. doi:10.16085/j.issn.1000-6613.2019-1182

Stasinakis, A. S., Thomaidis, N. S., Nikolaou, A., and Kantifes, A. (2005). Aerobic biodegradation of organotin compounds in activated sludge batch reactors. *Environ. Pollut.* 134 (3), 431–438. doi:10.1016/j.envpol.2004.09.013

Sun, S., Pang, S., Jiang, J., Ma, J., Huang, Z., Zhang, J., et al. (2018). The combination of ferrate(VI) and sulfite as a novel advanced oxidation process for enhanced degradation of organic contaminants. *Chem. Eng. J.* 333, 11–19. doi:10.1016/j.cej.2017.09.082

Tepong-Tsindé, R., Crane, R., Noubactep, C., Nassi, A., and Ruppert, H. (2015). Testing metallic iron filtration systems for decentralized water treatment at pilot scale. *Water* 7 (12), 868–897. doi:10.3390/w7030868

Tian, S. Q., Wang, L., Liu, Y. L., and Ma, J. (2020). Degradation of organic pollutants by ferrate/biochar: enhanced formation of strong intermediate oxidative iron species. *Water Res.* 183, 116054. doi:10.1016/j.watres.2020.116054

Wang, Q., Nakabayashi, M., Hisatomi, T., Sun, S., Akiyama, S., Wang, Z., et al. (2019). Oxysulfide photocatalyst for visible-light-driven overall water splitting. *Nat. Mater* 18 (8), 827–832. doi:10.1038/s41563-019-0399-z

Wang, R., Tang, T., Xie, J., Tao, X., Huang, K., Zou, M., et al. (2018). Debromination of polybrominated diphenyl ethers (PBDEs) and their conversion to polybrominated dibenzofurans (PBDFs) by UV light: mechanisms and pathways. *J. Hazard Mater* 354, 1–7. doi:10.1016/j.jhazmat.2018.04.057

Wang, Y., Li, X., Huang, Y., and Shen, J. (2013). Determination of organotin compounds by gas chromatography/mass spectrometry with derivatization-liquid-liquid extraction water supply & drainage. *J. Chromatogr. A* 49 (05), 28–32. doi:10.3969/j.issn.1002-8471.2013.05.006

Wang, Y., Xiao, Z., Liu, Y., Tian, W., Huang, Z., Zhao, X., et al. (2023). Enhanced ferrate(VI) oxidation of organic pollutants through direct electron transfer. *Water Res.* 244, 120506. doi:10.1016/j.watres.2023.120506

Wu, N., Liu, M., Tian, B., Wang, Z., Sharma, V. K., and Qu, R. (2023). A comparative study on the oxidation mechanisms of substituted phenolic pollutants by ferrate(VI) through experiments and density functional theory calculations. *Environ. Sci. Technol.* 57 (29), 10629–10639. doi:10.1021/acs.est.2c06491

Wu, S., Liu, H., Lin, Y., Yang, C., Lou, W., Sun, J., et al. (2020). Insights into mechanisms of UV/ferrate oxidation for degradation of phenolic pollutants: role of superoxide radicals. *Chemosphere* 244, 125490. doi:10.1016/j.chemosphere.2019.125490

Xiao, L., Wang, S., Zhou, Z., Wang, Y., and Zhang, Z. (2013). Research progress on the molecular mechanism of organotin-induced sexual distortion of marine gastropods. *J. Ecotoxicol.* 8 (03), 315–323+306. doi:10.7524/AJE.1673-5897.20130111001

Xiong, Z., Lai, B., Yuan, Y., Cao, J., Yang, P., and Zhou, Y. (2016). Degradation of p -nitrophenol (PNP) in aqueous solution by a micro-size Fe^0/O_3 process (m Fe^0/O_3): optimization, kinetic, performance and mechanism. *Chem. Eng. J.* 302, 137–145. doi:10.1016/j.cej.2016.05.052

Xu, H., Bai, Z., Zhao, H., Yang, L., and Deng, J. (2022). Research progress on preparation and application of methyltin. *Appl. Chem. Ind.* 51 (10), 2956–2959+2964. doi:10.3969/j.issn.1671-3206.2022.10.031

Yang, T., Wang, L., Liu, Y., Huang, Z., He, H., Wang, X., et al. (2019). Comparative study on ferrate oxidation of BPS and BPAF: kinetics, reaction mechanism, and the improvement on their biodegradability. *Water Res.* 148, 115–125. doi:10.1016/j.watres.2018.10.018

Yuan, G., Pi, R., Wu, Z., and Sun, X. (2020). Oxidative degradation of atrazine in water by ferrate-sulfite system Chemical Industry and Engineering Progress. *Chem. Industry Eng. Prog.* 39 (09), 3794–3800. doi:10.16085/j.issn.1000-6613.2019-1989

Zhang, L., Zhang, Z. C., and Cui, J. G. (2013). Simultaneous degradation of Cu(II) and Cr(VI) in the micro-polluted water by potassium ferrate. *Appl. Mech. Mater.* 295-298, 1191–1194. doi:10.4028/www.scientific.net/amm.295-298.1191

Zhang, S., Li, P., and Li, Z. H. (2021). Toxicity of organotin compounds and the ecological risk of organic tin with co-existing contaminants in aquatic organisms. *Comp. Biochem. Physiol. C Toxicol. Pharmacol.* 246, 109054. doi:10.1016/j.cbpc.2021.109054

Zhao, J., Wang, Q., Fu, Y., Peng, B., and Zhou, G. (2018). Kinetics and mechanism of diclofenac removal using ferrate(VI): roles of Fe^{3+}, Fe^{2+}, and Mn^2. *Environ. Sci. Pollut. Res. Int.* 25 (23), 22998–23008. doi:10.1007/s11356-018-2375-6

Zhao, Z., Xiang, L., Wang, Z., Liu, Y., Harindintwali, J. D., Bian, Y., et al. (2023). New insights into the Ferrate-Sulfite system for the degradation of polycyclic aromatic Hydrocarbons: a dual role for sulfite. *Chem. Eng. J.* 477, 147157. doi:10.1016/j.cej.2023.147157

Zhu, L., Zhang, Y., Chen, S., Xu, W., and Wang, P. (2019). Photocatalytic degradation of dimethyl phthalate in water by K_2FeO_4 and TiO_2 Chinese. *J. Environ. Eng.* 13 (10), 2369–2376. doi:10.12030/j.cjee.201811100